

Camouflaged Instance Segmentation In-The-Wild: Dataset And Benchmark Suite

Trung-Nghia Le¹, Yubo Cao², Tan-Cong Nguyen^{3,4}, Minh-Quan Le^{3,5}, Khanh-Duy Nguyen^{3,6}, Thanh-Toan Do⁷,
Minh-Triet Tran^{3,5,8}, and Tam V. Nguyen*²

¹National Institute of Informatics, Japan

²University of Dayton, US

³Vietnam National University, Ho Chi Minh City, Vietnam

⁴University of Social Sciences and Humanities, Ho Chi Minh City, Vietnam

⁵University of Science, Ho Chi Minh City, Vietnam

⁶University of Information Technology, VNU-HCM, Vietnam

⁷Monash University, Australia

⁸John von Neumann Institute, VNU-HCM, Vietnam

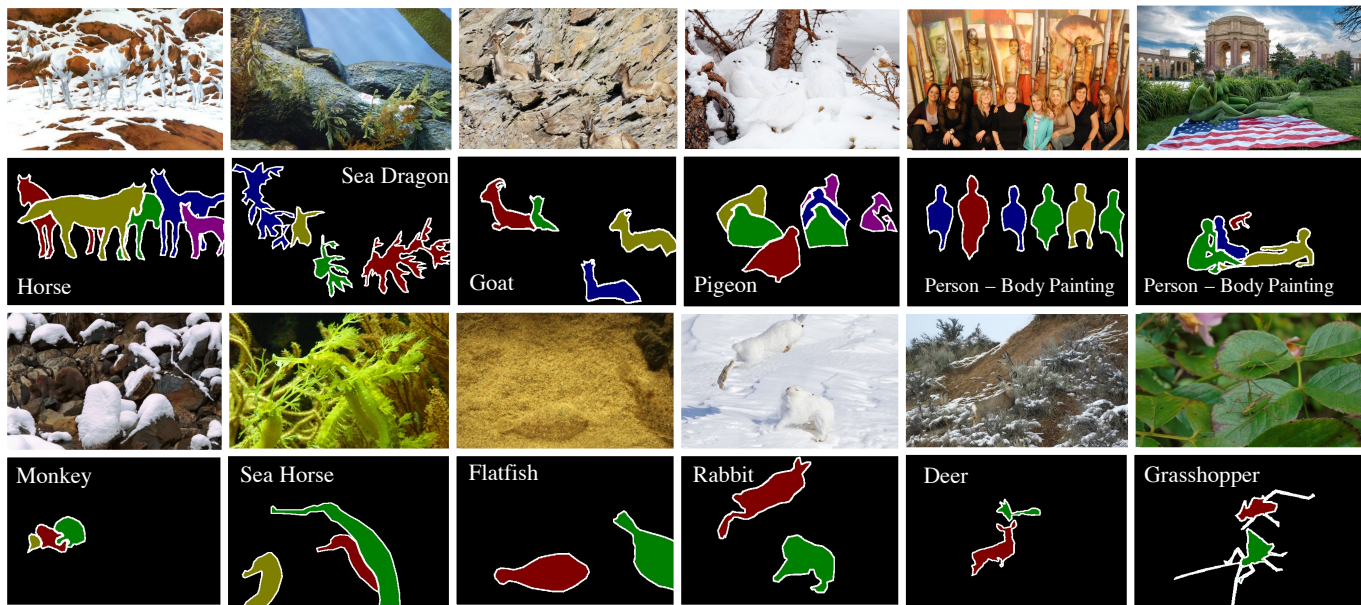


Fig. 1: A few examples from our **Camouflaged Object Plus Plus (CAMO++)** dataset with corresponding pixel-level annotations. Plus Plus (++) means the increment in terms of dataset size and the task compared to our preliminary CAMO dataset [1]. The first row is original images, followed by pixel-wise ground-truth. Each camouflaged instance is illustrated by a distinguished color for the visualization purpose only. Camouflaged instances attempt to conceal their texture into the background. Best viewed in color and with zoom.

Abstract—This paper pushes the envelope on camouflaged regions to decompose them into meaningful components, namely, camouflaged instances. To promote the new task of camouflaged instance segmentation in-the-wild, we introduce a new dataset, namely CAMO++, by extending our preliminary CAMO dataset (camouflaged object segmentation) in terms of quantity and diversity. The new dataset substantially increases the number of images with hierarchical pixel-wise ground-truths. We also provide a benchmark suite for the task of camouflaged instance segmentation. In particular, we conduct extensive evaluation of state-of-the-art instance segmentation methods on our newly constructed CAMO++ dataset in various scenarios. We also

propose Camouflage Fusion Learning (CFL) framework for camouflaged instance segmentation to further improve the state-of-the-art performance. The dataset, model, evaluation suite, and benchmark will be publicly available at our project page.¹

Index Terms—Camouflaged instance segmentation, in-the-wild, camouflage dataset, benchmark suite, multimodal

I. INTRODUCTION

The term “camouflage” was originally used to describe the behavior of an animal trying to hide itself from its surroundings to hunt or avoid being hunted [2], namely naturally

*Corresponding author. e-mail: tamnguyen@udayton.edu
Manuscript received August 06, 2020.

¹https://sites.google.com/view/ltnghia/research/camo_plus_plus

camouflaged objects [1]. Human adopted this and began to apply it widely on the battlefield. For example, soldiers and war equipment are applied with the camouflage effect by dressing or coloring their appearance to blend them with their surroundings, namely artificially camouflaged objects [1]. Autonomously identifying camouflaged objects is beneficial in various fields of computer vision (search-and-rescue work; wild species discovery and preservation [1], [3]), medical diagnostic (polyps detection and segmentation [4]; COVID-19 infection identification from lung x-ray [5]), media forensic (manipulated image/video detection and segmentation [6], [7]).

Early works of camouflage detection [8]–[15], which are based on handcrafted low-level features can work for only a few cases of simple and non-uniform background. Recently, deep learning based detectors [1], [16] have been proposed to tackle the problem of camouflaged object segmentation. However, these work can perform only at region-level, by mapping each pixel into camouflage/non-camouflage labels, which cannot show the number of camouflaged objects in the scene. None of them targets instance-level segmentation.

In this paper, we promote the new task of **camouflaged instance segmentation in-the-wild**. Camouflaged object is defined as all camouflaged pixels in an image without any further detail information such as the number of objects or semantic meaning [1]. In contrast, *camouflaged instance consists of only meaningful pixels, which cover an object instance*. To achieve this goal, the new task aims at *simultaneous decomposition of camouflaged regions into meaningful components, namely, camouflaged instances*. Camouflaged instance segmentation is more challenging than conventional camouflaged object segmentation in the sense that it *does not only map each pixels into labels but also assigns instance identity for pixels*. To our best knowledge, this is the first work to address camouflaged instance segmentation. Existing camouflaged object segmentation methods were developed with an assumption that camouflaged objects always exist in every images [16]–[18]. However this assumption is not always satisfied in practice. Meanwhile, *our work focuses on in-the-wild camouflage segmentation without any assumption*. To simulate the real-world, we aim to *segment camouflaged instances on unrestricted images, in which the camouflaged instances do not always exist*.

To this end, we introduce a new dataset specifically designed for the task of camouflaged instance segmentation. The proposed dataset contains 5500 images of human and more than 80 animal species with hierarchically pixel-wise annotation for all images. Our new dataset consists of both camouflage and non-camouflage images with the ratio of 50:50. It can be served as a benchmark for not only the camouflaged instance segmentation task, but also the conventional task of camouflaged object segmentation. We also provide a benchmark suite to facilitate the evaluation and advance the task of camouflaged instance segmentation. Particularly, we evaluate and analyze state-of-the-art instance segmentation methods in various scenarios. We remark that existing works [16]–[18] use only camouflage images to train and evaluate their methods with their assumption that camouflaged objects always exist in every images. In addition, existing camouflage datasets [1],

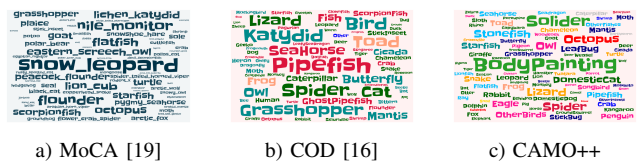


Fig. 2: Word cloud of category-distribution of camouflaged instances. Colors represent different meta-categories. Our CAMO++ dataset has 12 meta-categories while COD dataset has only 5 meta-categories.

[16] do not have ground-truth of non-camouflage images. It does not correspond to the real word since an animal or people are considered as camouflaged or not depending on the surrounding context. Therefore, we annotate both camouflage and non-camouflage image to utilize both image types for simulating the real-world. In addition, we propose a new fusion method to further improve the performance of the state-of-the-art methods.

We summarize the contribution of this paper as follows:

- We address the new task of **camouflaged instance segmentation in-the-wild** and analyze in-depth challenges of the problem. To our best knowledge, it is the first time that camouflaged instance segmentation is formally defined and explored. Finding camouflaged instances in scenes is a useful task and it can be an interesting problem for the community. A few existing work can perform only camouflaged object segmentation, but no current work focused on the instance-level. In addition, existing works are based on an assumption that camouflaged objects always exist, meanwhile our work performs segmentation on unrestricted images without any assumption.
- We present a new image dataset to promote the task of camouflaged instance segmentation. Our newly constructed **Camouflaged Object Plus Plus (CAMO++)** dataset, extended from our preliminary CAMO dataset [1], consists of 5,500 images of human and more than 90 animal species, including 2700 camouflage images and 2800 non-camouflage images. All images are hierarchically annotated with meta-category labels, fined-category labels, bounding-boxes, instance-level masks. Pixel-wise ground-truths are manually annotated for all instances in each image.
- We provide a benchmark suite for the task of camouflaged instance segmentation. In particular, we conduct extensive evaluation of state-of-the-art instance segmentation methods in various scenarios. We further provide in-depth analysis over the experiments. The CAMO++ dataset, evaluation suite, and benchmark will be made available on our website along with the publication².
- We propose Camouflage Fusion Learning (CFL) method for camouflaged instance segmentation to leverage the advantages of state-of-the-art methods in camouflaged instance segmentation.

The remainder of this paper is organized as follows. Section II summarizes the related work. Next, Section III intro-

²https://sites.google.com/view/ltnghia/research/camo_plus_plus

TABLE I: Statistics of camouflage datasets.

Dataset	Year	Publication	Type	#Img.	#Ann. Img.	#Obj. Cat.	#Ins. or #Obj.	Bbox. GT	Obj. Mask GT	Ins. Mask GT
CamouflagedAnimals [20]	2016	ECCV	Video	839	181	6	224	✗	✓	✓
CHAMELEON [21]	2018	-	Image	76	76	-	76	✗	✓	✗
CAMO [1]	2019	CVIU	Image	2,500	1,250	8	1,250	✗	✓	✗
COD [16]	2020	CVPR	Image	10,000	5,066	69	5,930	✓	✓	✓
MoCA [17]	2020	ACCV	Video	37,250	7,617	67	7,617	✓	✗	✗
CAMO++	2020	-	Image	5,500	5,500	93	32,756	✓	✓	✓

duces the constructed CAMO++ dataset. Section IV presents our proposed Camouflage Fusion Learning framework for camouflaged instance segmentation. Section V then reports benchmark suite and evaluation of baselines on the newly constructed dataset. Finally, Section VII draws the conclusion and paves the way for future work.

II. RELATED WORK

A. Camouflaged Object Segmentation

A camouflaged object is defined as all camouflaged pixels in an image without any further detail information such as the number of objects or semantic meaning [1]. Although camouflaged object recognition also has a wide range of applications, in the literature, this research field has not been well explored in the literature. Early works related to camouflage had been dedicated to detecting the foreground region even when some of their texture is similar to the background [8]–[10]. These works distinguish foreground and background based on simple features such as color, intensity, shape, orientation, and edge. A few methods based on handcrafted low-level features are proposed to tackle the problem of camouflage detection [11]–[15]. However, all these methods work for only a few cases of simple and non-uniform background, thus their performances are unsatisfactory in camouflaged object segmentation due to strong similarity between the foreground and the background.

Recently, Le *et al.* [1] proposed an end-to-end network, dubbed ANet, for camouflaged object segmentation through integrating classification information into segmentation. The potential idea of utilizing classification into segmentation can be useful when applying for multiple regional segmentation in appropriate ways. Following the same direction, Fan *et al.* [16] later developed SINet which includes two main modules, namely the search module and the identification module. This work is based on simulated hunting, where a predator will first judge whether a potential prey exists, *i.e.*, it will search for a prey; then, the target animal can be identified; and, finally, it can be caught. In the recent work, Yan *et al.* [22] recently introduced MirrorNet, a dual stream network, which possesses the main stream and the mirror stream. This bio-inspired network effectively captures different layouts of the scene to boost up the segmentation accuracy. Jinchao *et al.* [18] proposed TINet, which interactively refines multi-level texture and segmentation features to gradually enhance segmentation of camouflaged objects. According to our best of knowledge, no existing work has been proposed for camouflaged instance segmentation until the day.

B. Camouflage Datasets

Table I summarizes the main characteristics of different datasets in camouflage research. CamouflagedAnimals [20] and CHAMELEON [21] are two first camouflage dataset with mask annotations. However, these dataset have small number of images, which is not enough to train deep learning methods. Le *et al.* [1] built CAMO dataset, the first camouflage dataset with more than 1000 annotated images. The CAMO dataset consists of 1250 images, a limited number of samples to train and evaluate deep learning methods. Later, Fan *et al.* [16] collected COD dataset, which comprises 10,000 images for both camouflage and non-camouflage. However, they annotated only 5,000 camouflage images. Lamdouaret *et al.* [17] recently developed MoCA dataset for the task of camouflage object detection, thus the dataset contain only bounding box ground-truth. Although CAMO [1] and COD [16] were constructed with multiple levels of ground-truth, they have been only used for the camouflaged object-level segmentation problem. To our best of knowledge, our newly constructed CAMO++ dataset is the very first dataset fully supporting for camouflaged instance-level segmentation in-the-wild.

C. Instance Segmentation

Instance segmentation is the task of unifying object detection and semantic segmentation. It has been intensively studied in recent years where the segmentation based approach or the proposal based approach is employed. The segmentation based approach [23]–[27] generally adopts two-stage processing: segmentation first and then instance clustering. The proposal based approach [28]–[30], on the other hand, predicts bounding-boxes first and then parses the bounding-boxes to obtain mask regions [28] or exploits object detection models (*e.g.*, Faster RCNN [31] or R-FCN [32]) to classify mask regions [29], [30]. Proposal based methods, which achieve state-of-the-art performance, have gained popularity due to more advantages than segmentation based methods. Hence, this paper solely focuses on proposal based approaches.

Proposal-based methods are categorized into single-stage and two-stage approaches. Two-stage methods follow detect-then-segment approach. These methods first perform object detection to extract bounding-boxes around each instance object, and then perform binary segmentation inside each bounding-box to separate the foreground (object) and the background. Two-stage methods (*e.g.*, Mask RCNN [29] and its variants) are quite slow and precludes the use of many real-time applications. Mask RCNN [29], the first end-to-end model for instance segmentation, is extended from Faster RCNN [31] by adding a branch for predicting an object

mask in parallel with the existing branch for bounding-box detection. Mask Scoring RCNN (MS RCNN) [33], Cascade Mask RCNN [34], and PANet [35] are extended from Mask RCNN to improve the quality of segmented instances. MS RCNN [33] contains a network block on top of Mask RCNN to learn the quality of the predicted instance masks. Meanwhile, Cascade Mask RCNN [34], a multi-stage architecture, consists of a sequence of detectors trained with increasing Intersection over Union (IoU) thresholds, to be sequentially more selective against close false positives. PANet [35] aims at boosting information flow in feature extractor through bottom-up path augmentation.

Single-stage methods are inspired by anchor-free object detection methods (such as CenterNet [36] and FCOS [37]). Generally these methods are faster than two-stage methods. Some of them can even run in real-time. YOLACT [38] is one of the first methods attempting real-time instance segmentation. YOLACT breaks instance segmentation into two parallel subtasks (*i.e.*, generating a set of prototype masks and predicting per-instance mask coefficients), and then linearly combines the prototypes with the mask coefficients. BlendMask [39] and CenterMask [40] are extended from YOLACT. These methods aim to blend cropped prototype masks with a finer-grained mask within each bounding-box. CenterMask [40] adds a spatial attention-guided mask branch to anchor-free one stage object detector (FCOS [37]). BlendMask [39] first predicts dense per-pixel position-sensitive instance features with very few channels, and then merges attention maps for each instance through a blender module. In addition, PolarMask [41] formulates the instance segmentation problem as predicting contour of instance through instance center classification and dense distance regression in a polar coordinate. Meanwhile, EmbedMask [42] generates embeddings for pixels and proposals to assign pixels to the mask of the proposal if their embedding are similar. TensorMask [43] investigates the paradigm of dense sliding window instance segmentation, using structured 4D tensors to represent masks over a spatial domain. In addition, RetinaMask [44] is proposed by adding a novel instance mask prediction head to the single-shot RetinaNet [45] detector. On the other hand, FCIS [30] and CondInst [46] utilize fully convolutional networks to produce masks. SOLO [47] reformulates the instance segmentation as category prediction and mask generation to directly output masks without computing bounding boxes.

According to our best of knowledge, no existing work has been proposed for camouflaged instance segmentation officially. Obviously we notice the lack of a large-scale dataset for the training and testing purposes. Therefore, in this paper, we build a benchmark for the task of camouflaged instance segmentation by training instance segmentation methods on our newly constructed CAMO++ dataset. We further conduct extensive evaluation of state-of-the-art instance segmentation methods in various scenarios.

III. CAMOUFLAGED INSTANCE DATASET

The core contribution of this paper is our CAMO++ dataset extending our preliminary CAMO dataset [1]. This new large-



Fig. 3: A few examples of non-camouflage images. Each instance is overlaid by a distinguished color for the visualization purpose only. Best viewed in color and with zoom.

TABLE II: Distribution of data in CAMO++ dataset.

	Training	Testing	Total
Camouflage Images	1,700	1,000	2,700
Non-camouflage Images	1,800	1,000	2,800
Instances	17,735	15,021	32,756

scale dataset enables us to train and evaluate state-of-the-art methods for the task of camouflaged instance segmentation.

A. Dataset Construction

1) *Camouflage Image Collection*: We initially collected 4000 images in which at least one camouflaged object exists. We collected the images of camouflaged objects from the Internet with different keywords by combining adjective “camouflaged”, “concealed”, “hidden”, with various animals (*e.g.*, cat, dog, seahorse, *etc.*), persons (*e.g.*, soldier, body-painting, *etc.*), and environments (*e.g.*, marine, underwater, mountain, desert, forest, *etc.*).

Then, we manually discarded images with low resolution. We later mixed them with 1250 camouflage images from our preliminary CAMO dataset [1] and manually discarded duplication. Finally, we ended up with 2700 images.

We asked ten annotators to differentiate camouflaged instances and annotate these instances in all images individually using a custom-designed interactive segmentation tool. On average, each person takes 5-20 minutes to annotate one image depending on its complexity. The annotation stage spanned few months. The outcome of this process is the binary mask and its hierarchical categories for each instance (*c.f.* Figure 1).

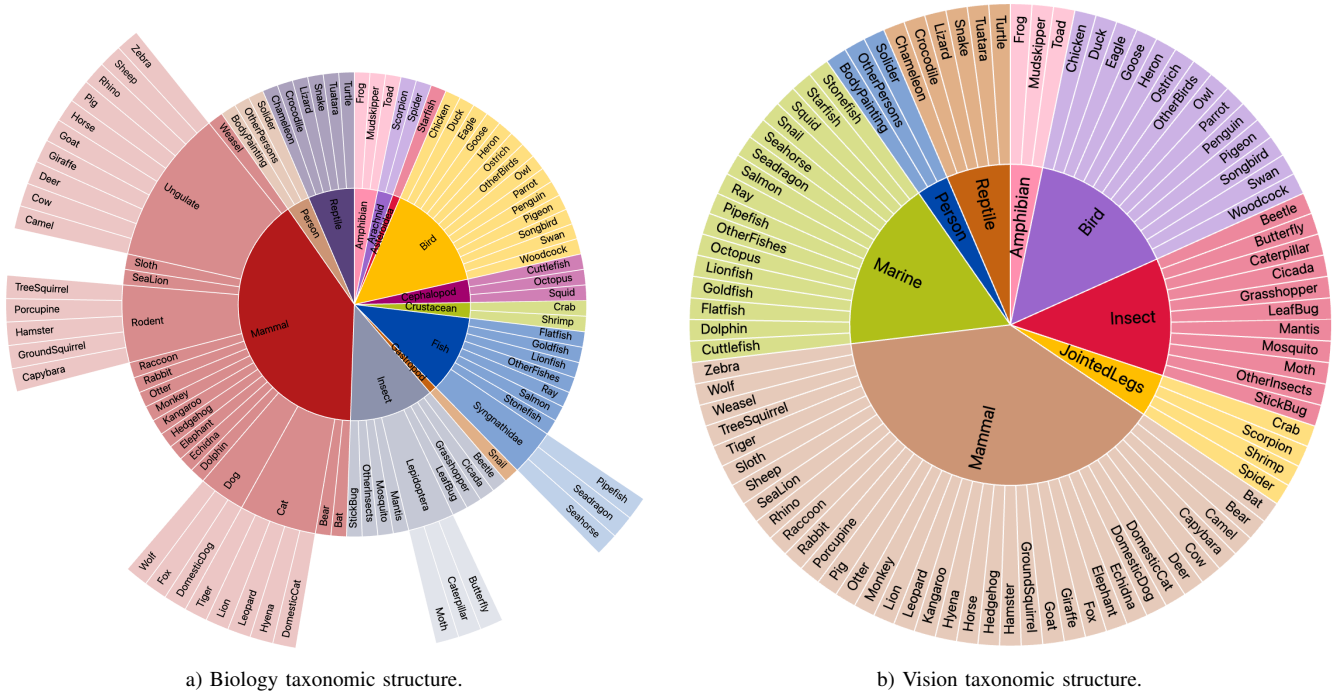


Fig. 4: Hierarchical taxonomic structure in our proposed CAMO++ dataset.

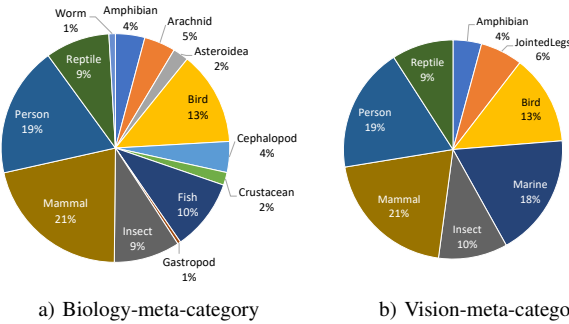


Fig. 5: Distribution of camouflage meta-categories in CAMO++ dataset.

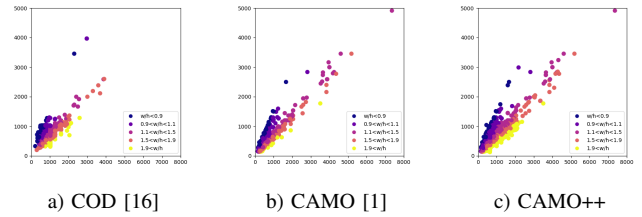


Fig. 6: Image resolution distribution.

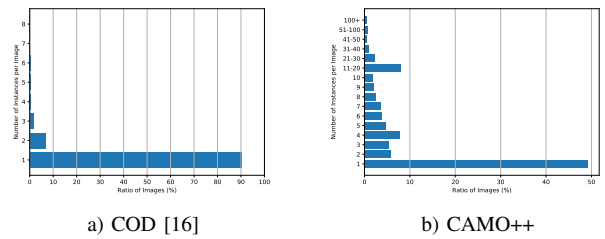


Fig. 7: The density of instances of datasets.

2) *Non-Camouflage Image Collection*: We manually select 2800 images from the LVIS dataset [48], which contains at least a human or animal instance. We manually selected the images to guarantee they do not contain any camouflaged instances for false positive segmentation. Figure 3 shows examples of the non-camouflage images.

3) *Dataset Splits*: We randomly split 2,700 camouflage images into separate training and testing sets, in which the training set consists of 1,700 images, and the testing set consists of 1,000 images. We also randomly split 2,700 non-camouflage images into training and testing sets with 1,800 images and 1000 images, respectively.

B. Dataset Specifications and Statistics

We describe in this section the **Camouflaged Object Plus Plus (CAMO++)** dataset designed explicitly for the task of camouflaged instance segmentation. ++ means the increment in terms of dataset size and the task compared to our previous

CAMO dataset [1]. Some examples are shown in Figure 1 with the corresponding ground-truth label annotations. As shown in Table I, our CAMO++ dataset has the highest number of object categories and object instances. Note that COD dataset [16] only provides the ground-truth of camouflaged instance, that does not satisfy the in-the-wild setting in nature.

Category Diversity. In CAMO++, we focus on various camouflaged pieces. Figure 4a highlights diversity in biology-inspired hierarchical categorization. The CAMO++ dataset consists of 12 biological meta-categories (e.g., amphibian, arachnid, asteroidea, bird, cephalopod, crustacean, fish, gas-

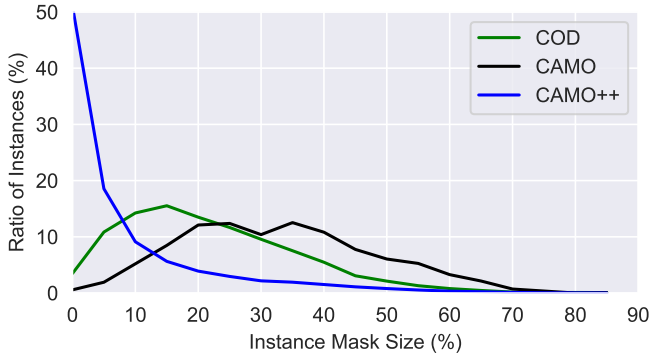


Fig. 8: Distribution of the instance size. CAMO++ dataset contains more small objects than other datasets. Size of camouflaged instances in CAMO++ dataset is diversity (*i.e.*, tiny, small, medium, large).

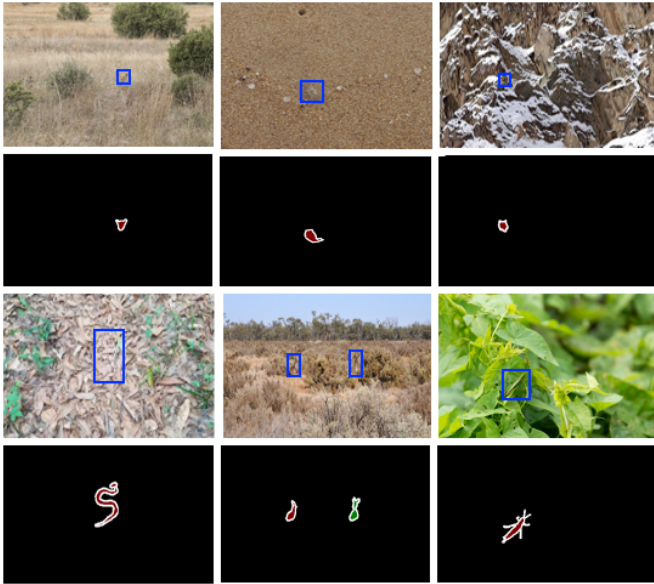


Fig. 9: Examples of tiny camouflaged instances. Each instance is overlaid by a distinguished color for the visualization purpose only. Best viewed in color and with zoom.

tropod, insect, mammal, person, and reptile) and 93 categories (*c.f.* Figure 4a). Each category contains 352 instances on average. Figure 5a shows ratio of biological meta-categories in the CAMO++ dataset, where each biology-meta-category contains 2,730 instances on average. Figure 2 shows the word cloud of the category distribution of camouflaged instances in different datasets.

However, biological categorization is generally complicated for machines, and even to computer vision community, to understand. Therefore, we re-organized categories based on vision features (*i.e.*, appearance) in combination with biological features (*i.e.*, behavior, living environment). We built a new list of 8 meta-categories (*e.g.*, amphibian, jointed legs, bird, marine, insect, mammal, person, reptile) (*c.f.* Figure 4b). The ratios for vision-meta-categories are shown in Figure 5b, in which each vision-meta-category contains 4,095 instances

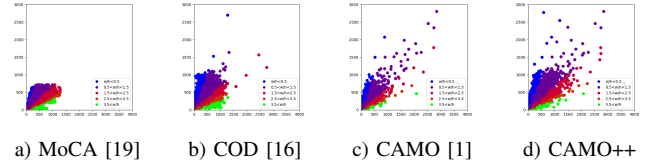


Fig. 10: Instance bounding box distribution of different camouflaged datasets.

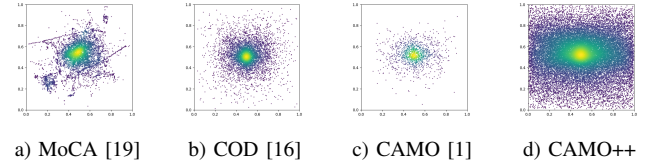


Fig. 11: Instance center bias of existing datasets.

on average.

Our CAMO++ dataset contains more object categories and meta-categories than existing datasets. CAMO++ dataset has 93 categories and 12 meta-categories in compared with 69 categories and 5 meta-categories of COD dataset [16], and 67 categories of MoCA dataset [17] (*c.f.* Table I). The diversity of CAMO++ dataset enables a comprehensive understanding of camouflage instances in both biology and computer vision communities.

Image Resolution. Figure 6 illustrates the image resolution distribution of different datasets. As seen in the figure, CAMO++ dataset has the diversity in the image resolution. In addition, CAMO++ has more high-resolution images than COD dataset [16].

Instance Density. In CAMO++ dataset, each image has from 1 to more than 100 instances. Our CAMO++ dataset has 6.0 instances per image on average, while COD dataset [16] has only 1.2 instances per image and maximum of 8 instances. Figure 7 illustrates ratios of number of instances in an image over the CAMO++ dataset. It is noteworthy that a large number of images with multiple instances, including separate single instances and spatially connected/overlapping instances, take 51% of the CAMO++ dataset. 38% of the images have from 2 to 10 instances. 10% of the images contain from 11 to 30 instances. The remainder, 3% of images, is with more than 30 instances. In contrast, only 10% images of COD dataset [16] has multiple single instances (*c.f.* Figure 7). This makes our CAMO++ dataset more challenging for the camouflaged instance segmentation task.

Instance Size. The size of an instance is defined as the proportion of its pixels to the entire image. Figure 8 shows distribution of the instance size. The CAMO++ dataset contains a large number of small and medium instances. Small instance with the size smaller than 0.1 takes ratio of 69.6%, and medium instances with size from 0.1 to 0.3 take ratio of 23.8%. Meanwhile, COD dataset [16] contains 14.3% of small instances and 64.5% of medium instances. It is also noteworthy that CAMO++ dataset consists of a fair amount of tiny instances (*c.f.* Figure 9), which makes our dataset more challenging for the task of camouflaged instance segmentation.

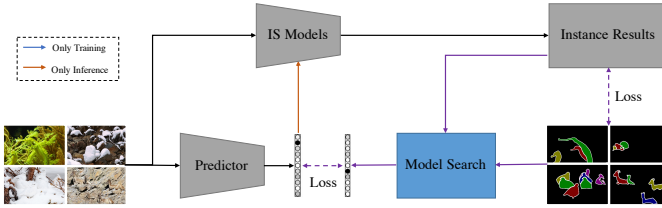


Fig. 12: Workflow of our Camouflage Fusion Learning (CFL) for camouflaged instance segmentation. IS stands for instance segmentation.

In addition, instance bounding box distributions in Figure 10 show the broader range of bounding box sizes in our CAMO++ dataset, compared with existing datasets.

Center Bias. Figure 11 depicts the distributions of object centers in normalized image coordinates over all images in camouflage dataset. Camouflage instances are biased to the center of images on all dataset. This can be explained that camouflage images are usually cropped for camouflaged instances nearly at the center for people to identify those concealed instances, even for videos (*i.e.*, MoCA dataset [19]). Unlike existing datasets, instances in CAMO++ dataset localize over the entire image.

The newly constructed CAMO++ dataset also inherits challenging attributes from our previous CAMO dataset [1], such as *object appearance, background clutter, shape complexity, object occlusion, and distraction*. Readers please refer to the CAMO dataset [1] for more details.

IV. CAMOUFLAGE FUSION LEARNING

A. Proposed Framework

1) *Overview:* General instance segmentation methods [29], [33] can be applied for camouflaged instance segmentation by fine-tuning models on camouflage datasets. However, they are imperfect in the sense that each method may have advantages on specific contexts but disadvantages on others. To utilize the strength of each individual instance segmentation methods, we propose a simple yet efficient Camouflage Fusion Learning (CFL) to fuse various models by learning image contexts.

Figure 12 depicts our proposed Camouflage Fusion Learning for camouflaged instance segmentation. We first train instance segmentation methods on our CAMO++ dataset independently (*c.f.* Section V-A). We then generate results of all instance segmentation models and then search results corresponding with the best model for each image. Algorithm 1 outlines our Model Search algorithm. We later train a model predictor to predict the best instance segmentation model for each image.

2) *Objective Function:* Given an image x with corresponding instance ground-truth y , predictor f , and M instance segmentation models, our loss function includes two parts as follows:

$$\mathcal{L} = \mathcal{L}_{pred}(f(x), c) + \sum_{g \in M} \mathcal{L}_{ins}^g(g(x), y), \quad (1)$$

where \mathcal{L}_{pred} is model prediction loss, c is the best model chosen, and \mathcal{L}_{ins}^g denotes instance segmentation loss following

Algorithm 1 Model Search

Input: :

- 1) List of instance segmentation results $ins[N \times K]$ of K models on N images.
- 2) Ground-truth $gt[N \times 1]$ of N images.

Output: Results $pred[N \times 1]$ of N images.

- 1: $pred \leftarrow \emptyset$
- 2: **for** $i \leftarrow 1$ to N **do**
- 3: $k \leftarrow \underset{k \in K}{\operatorname{argmax}}(\mathbf{AP}(gt[1 : i], pred \cup ins[i, k]))$
- 4: $pred \leftarrow pred \cup ins[i, k]$
- 5: **return** $pred$

the employed instance segmentation model g . The multinomial cross entropy loss was employed for \mathcal{L}_{pred} .

3) *Implementation:* We employed Vision Transformer (ViT-Base16) [49] as the model predictor. Five well-known instance segmentation methods: Mask RCNN [29], Cascade Mask RCNN [34], MS RCNN [33], RetinaMask [44], and CenterMask [40] were empirically chosen for our CFL. All methods were developed on PyTorch, using publicly available source codes provided by the authors.

B. Training Strategy

Our CFL was trained on two stages. In the first stage, instance segmentation models were trained independently with their loss \mathcal{L}_{ins} (*c.f.* Section V-A). In the second stage, we froze instance segmentation models and trained the model predictor using the loss \mathcal{L}_{pred} .

The predictor training process is conducted by fine-tuning the ImageNet pre-trained model on our CAMO++ dataset. We proposed 5-fold stratified sampling for training strategy. In particular, we randomly split training data into training set (4 folds) and validation set (1 fold) to avoid overfitting. We also applied simple augmentations such as resizing, cropping, translation, rotation, flipping. We set the size of each mini-batch to 16 and used AdamW optimization with a weight decay of 0.001 and moments $\beta_1 = 0.9$ and $\beta_2 = 0.0.999$. Our model predictor ViT was trained for 100 epochs with batch size of 16, base learning rate of 0.0008, warmup of 1000 steps and cosine learning rate decay.

We trained models on PCs with 64GB RAM memory and Tesla P100 GPUs. The training code and trained model will be published upon the acceptance of this paper.

V. BENCHMARK SUITE

A. Baseline Methods

In addition to our large-scale CAMO++ database, we conduct a competitive benchmark for camouflaged instance segmentation. To this end, we trained and tested various instance segmentation methods (*i.e.*, Mask RCNN [29], Cascade Mask RCNN [34], MS RCNN [33], RetinaMask [44], YOLACT [38], CenterMask [40], SOLO [47], and BlendMask [39],) on subsets as in Section III-A3. Figure 13 shows the timeline of the benchmarked state-of-the-art methods.

TABLE III: The results of setting 1: Camouflaged instances does not always exist. The best results for each type of backbone are shown in **green**, **red**, and **blue**, respectively.

Method	Backbone	Average Precision (AP)			AP Across Scales			Average Recall (AR)			AR Across Scales		
		AP	AP ₅₀	AP ₇₅	AP _S	AP _M	AP _L	AR ₁	AR ₁₀	AR ₁₀₀	AR _S	AR _M	AR _L
Mask RCNN [29]	ResNet50-FPN	16.1	36.4	12.9	4.0	19.0	34.1	14.7	22.3	24.3	6.4	28.6	46.0
Mask RCNN [29]	ResNet101-FPN	17.1	37.6	14.5	4.7	20.5	35.3	15.5	23.1	25.3	6.8	31.0	47.1
Mask RCNN [29]	ResNeXt101-FPN	19.9	42.2	16.7	6.8	22.5	39.7	18.5	25.2	27.0	8.4	31.4	50.2
Cascade Mask RCNN [34]	ResNet50-FPN	16.9	36.6	13.9	3.6	20.0	35.8	15.5	23.5	25.6	5.3	30.5	48.3
Cascade Mask RCNN [34]	ResNet101-FPN	17.6	37.9	15.0	4.7	21.6	37.0	15.9	24.3	26.7	8.8	31.6	50.0
Cascade Mask RCNN [34]	ResNeXt101-FPN	21.5	44.0	19.7	6.3	26.1	40.3	18.6	28.8	32.0	11.9	39.2	55.2
MS RCNN [33]	ResNet50-FPN	19.1	38.1	18.0	8.3	23.2	35.4	15.5	23.0	25.9	12.1	31.3	44.9
MS RCNN [33]	ResNet101-FPN	20.0	38.4	18.9	8.6	24.6	37.2	16.2	24.1	26.9	12.5	33.3	47.2
MS RCNN [33]	ResNeXt101-FPN	22.9	44.2	21.8	11.8	27.8	39.9	18.0	26.9	30.5	14.6	37.1	50.2
RetinaMask [44]	ResNet50-FPN	17.4	37.5	14.5	8.8	21.8	32.9	15.1	23.8	27.7	12.5	33.6	46.3
RetinaMask [44]	ResNet101-FPN	18.0	38.2	15.7	10.3	22.2	33.9	16.1	24.9	28.5	18.1	35.6	47.8
RetinaMask [44]	ResNeXt101-FPN	20.0	41.2	17.6	12.4	24.9	36.9	17.8	26.6	30.4	16.6	38.0	50.5
YOLOACT [38]	ResNet50-FPN	14.7	31.4	12.9	5.1	19.8	32.8	14.7	20.9	22.8	11.5	29.2	43.9
YOLOACT [38]	ResNet101-FPN	15.9	32.4	14.2	8.6	19.6	36.1	16.1	22.2	23.6	13.0	28.1	47.1
CenterMask [40]	ResNet50-FPN	14.9	34.9	11.1	9.5	18.6	27.5	13.3	22.9	26.6	14.5	34.8	43.2
CenterMask [40]	ResNet101-FPN	15.9	35.7	12.8	8.8	19.4	29.9	14.8	23.5	26.1	14.5	33.6	44.5
CenterMask [40]	ResNeXt101-FPN	19.9	42.4	17.5	9.0	24.4	33.9	16.9	26.8	30.3	15.2	38.5	47.7
SOLO [47]	ResNet50-FPN	14.8	29.7	13.6	6.3	20.6	31.6	13.9	21.4	23.8	8.8	31.0	45.9
SOLO [47]	ResNet101-FPN	18.3	36.2	16.5	5.9	22.5	35.0	17.3	25.5	27.4	12.2	33.5	49.5
SOLO [47]	ResNeXt101-FPN	19.3	37.3	18.2	9.3	21.1	37.5	18.7	26.8	28.6	12.0	33.2	52.7
BlendMask [39]	ResNet50-FPN	18.2	38.6	15.4	9.8	23.7	34.1	15.9	24.7	28.6	15.3	35.7	47.7
BlendMask [39]	ResNet101-FPN	20.3	40.6	18.2	12.1	26.5	38.1	17.3	25.6	28.9	14.9	36.7	50.9
Our CFL	ResNet50-FPN	19.2	39.0	16.5	3.1	21.8	40.8	17.5	25.4	27.9	7.9	34.2	50.0
Our CFL	ResNet101-FPN	21.9	41.9	21.2	7.3	25.5	43.6	18.5	26.9	29.2	12.2	36.1	52.0
Our CFL	ResNeXt101-FPN	25.1	47.2	24.1	5.1	29.2	47.0	21.0	29.8	33.1	11.8	40.5	55.9

To demonstrate the generalization of methods, we employ different backbones, namely, ResNet50-FPN [50], ResNet101-FPN [50], and ResNeXt101-FPN [51], for each instance segmentation methods. For YOLOACT and BlendMask, we used only ResNet50-FPN and ResNet101-FPN backbones because these methods previously have not been implemented on ResNeXt101-FPN backbone [38], [39].

We trained models on PCs with 64GB RAM memory and Tesla P100 GPUs. Methods were fine-tuned from the MS-COCO pre-trained models using default public configurations provided by authors.

B. Evaluation Measures

All reported results follow standard COCO-style Average Precision (AP) metrics that include AP (averaged over IoU thresholds from 50% to 95%), AP_{50} (AP for IoU threshold 50%), AP_{75} (AP for IoU threshold 75%) [52]. We also evaluated results using AP at different scales (AP_S , AP_M , AP_L), where S, M, and L represent small (the area is below 32*32 pixels), medium (the area is from 32*32 to 96*96 pixels) and large objects (the area is above 96*96 pixels), respectively.

We also reported results on Average Recall (AR) metrics that include AR_1 , AR_{10} , AR_{100} (AR given number of detection per image) [52]. Similar to AP, we also evaluated results using AR at different scales (AR_S , AR_M , AR_L).

C. Benchmarking Results

We evaluate instance segmentation methods on different settings, namely:

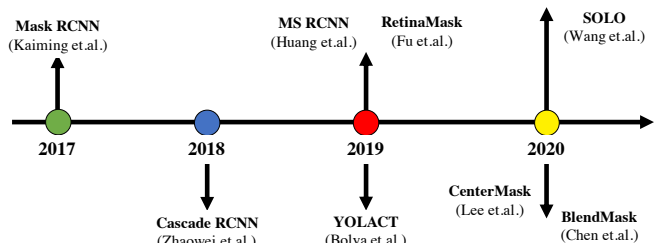


Fig. 13: Timeline of benchmarked instance segmentation methods.

- Setting 1: This experimental setting simulates the real-world (*i.e.*, in-the-wild or unrestricted images), where camouflaged instances do not always exist in images. We train and test models on all images.
- Setting 2: This experimental setting assumes that camouflaged instances appear in every images. We train and test models on only images containing camouflaged instances.

The detailed performance is discussed in the subsections below.

1) **Setting 1 (Camouflaged Instances Does Not Always Exist)**: Table III details the performance of different methods on the first experimental setting: segment multiple camouflaged instance on unrestricted images. As can be seen from the table, the better backbones tend to produce better results within the same methods. ResNeXt101-based implementations provide the best performance. In terms of Average Precision (AP), AP_{50} metrics obviously obtain the highest scores. On the con-

TABLE IV: The results of setting 2: Camouflaged instances appear in every images. The best results for each type of backbone are shown in **green**, **red**, and **blue**, respectively.

Method	Backbone	Average Precision (AP)			AP Across Scales			Average Recall (AR)			AR Across Scales		
		AP	AP ₅₀	AP ₇₅	AP _S	AP _M	AP _L	AR ₁	AR ₁₀	AR ₁₀₀	AR _S	AR _M	AR _L
Mask RCNN [29]	ResNet50-FPN	24.4	52.5	21.1	6.5	18.7	26.3	26.7	33.1	33.1	6.7	25.1	35.7
Mask RCNN [29]	ResNet101-FPN	23.7	51.5	19.6	7.0	16.2	26.0	26.3	32.0	32.1	7.8	23.8	34.7
Mask RCNN [29]	ResNeXt101-FPN	31.2	62.7	29.4	8.6	22.3	34.1	32.8	38.6	38.7	11.7	28.1	42.0
Cascade Mask RCNN [34]	ResNet50-FPN	25.1	51.8	21.9	4.8	17.4	27.7	27.0	34.4	34.5	4.4	24.7	37.7
Cascade Mask RCNN [34]	ResNet101-FPN	26.7	53.8	23.6	11.4	18.9	29.2	28.8	36.5	36.5	12.2	25.8	39.8
Cascade Mask RCNN [34]	ResNeXt101-FPN	33.6	66.0	30.7	11.7	25.0	36.5	34.0	44.6	45.0	13.9	35.0	48.2
MS RCNN [33]	ResNet50-FPN	27.0	54.3	24.5	11.7	19.6	29.3	27.5	33.4	3.5	1.33	26.1	35.8
MS RCNN [33]	ResNet101-FPN	28.1	55.6	26.2	9.3	21.7	30.2	29.0	35.0	35.4	10.0	27.7	37.8
MS RCNN [33]	ResNeXt101-FPN	31.0	60.4	29.2	8.0	24.2	33.2	32.4	38.4	38.6	10.0	29.8	41.5
RetinaMask [44]	ResNet50-FPN	21.5	48.2	17.0	14.4	18.5	2.8	25.9	31.5	31.9	16.1	25.6	33.9
RetinaMask [44]	ResNet101-FPN	23.5	50.2	19.5	13.9	20.3	24.9	27.4	33.7	33.9	20.0	28.6	35.6
RetinaMask [44]	ResNeXt101-FPN	25.8	53.1	23.3	13.3	20.5	27.8	29.9	36.6	36.8	13.9	28.7	39.3
YOLACT [38]	ResNet50-FPN	20.6	41.9	17.5	6.5	16.3	22.3	25.8	29.3	29.6	9.4	21.8	32.0
YOLACT [38]	ResNet101-FPN	21.7	42.1	20.0	6.2	17.2	23.5	25.9	30.1	30.1	7.2	22.8	32.4
CenterMask [40]	ResNet50-FPN	19.7	47.1	13.7	6.7	13.8	21.4	22.9	30.7	30.9	11.0	26.8	32.3
CenterMask [40]	ResNet101-FPN	23.1	53.3	17.1	9.3	16.3	25.2	26.8	34.9	35.2	26.1	29.0	37.0
CenterMask [40]	ResNeXt101-FPN	26.6	57.4	23.2	7.7	17.0	29.6	29.8	37.1	37.3	10.0	28.7	40.0
SOLO [47]	ResNet50-FPN	22.6	46.9	19.3	6.0	8.9	26.5	26.2	28.9	29.0	6.1	13.2	33.6
SOLO [47]	ResNet101-FPN	23.8	48.5	21.3	6.9	12.0	27.3	28.4	30.9	31.0	7.8	15.9	35.4
SOLO [47]	ResNeXt101-FPN	24.3	48.5	22.1	5.8	9.0	28.7	28.9	31.2	31.3	8.3	13.1	36.5
BlendMask [39]	ResNet50-FPN	21.7	47.4	18.3	10.3	17.0	23.4	26.1	31.4	31.5	14.4	24.4	33.6
BlendMask [39]	ResNet101-FPN	25.5	53.5	20.6	18.8	20.2	27.3	30.2	35.5	35.6	22.2	26.9	38.1
Our CFL	ResNet50-FPN	35.2	66.3	32.6	6.3	25.9	38.2	32.5	39.6	39.8	8.3	31.0	42.7
Our CFL	ResNet101-FPN	36.9	68.2	34.7	15.4	27.0	39.9	34.1	42.2	42.7	22.8	33.6	45.4
Our CFL	ResNeXt101-FPN	42.8	75.9	44.6	17.2	32.5	46.1	38.8	47.9	48.3	21.7	37.8	51.5

trary, AP₇₅ metrics yield the lowest scores. Meanwhile, AP_L, AR₁₀₀, AR_L produce the highest scores in terms of AP Across Scales, Average Recall, and AR Across Scales, respectively. In general, the benchmarking methods consistently perform across the performance metrics. In other words, the methods performing well in one performance metrics tend to perform well for the rest.

We later take a closer look to the performance of compared instance segmentation methods. Our CFL achieved the SOTA performances across all metrics. CFL significantly outperformed all other instance segmentation methods with AP of 19.2, 21.9, 25.1 on backbones ResNet50-FPN, ResNet101-FPN, ResNeXt101-FPN, respectively. Our method was also consistently better than other competitors in terms of AR.

2) Setting 2 (Camouflaged Instances Always Exist):

Table IV reports the performance of different methods on the second experimental setting with the assumption that camouflaged objects always exist in all image. Again, CFL consistently significantly outperformed other competitors. Our method obtained the best performance across all metrics. In particular, it achieved the SOTA performances with AP of 35.2, 36.9, 42.8 on backbones ResNet50-FPN, ResNet101-FPN, ResNeXt101-FPN, respectively.

3) *Qualitative Comparison*: Figure 14 shows the visual comparison of different methods with the same ResNet50 backbone. We remark that we visualize only ResNet50 backbone since this backbone is most popular in segmentation methods.

As illustrated in the figure 14, our CFL yields better results than all other methods. Our results are close to the ground

truth. Our CFL is able to segment camouflaged instances with fine details, demonstrating its robustness. CFL can well handle a variety of challenging cases such as camouflaged instances have similar color and texture with the background, shape complexity, multiple objects, etc.

4) *Failure Cases and Discussion*: In this subsection, we discuss about the failure cases of our CFL in camouflaged instance segmentation. Figure 15 shows the exemplary failure cases in CAMO++ dataset. As can be seen from the figure, the method struggles to localize and segment camouflaged instances due to tiny size (the first row) or extreme resemblance to the background (the second row). As also shown in Figure 15, these cases are immensely challenging examples, even for human. We also observe the failure cases on occluded or overlapping camouflaged instances (the last row), which cause wrong segmentation (the bottom left example) or misclassification between camouflaged instances and non-camouflaged instances (the bottom right example).

From the visualization and aforementioned observation along with experimental results, even the leading instance segmentation methods in the deep learning era remain limited and cannot yet effectively segment multiple camouflaged instances on unrestricted images without any assumption (Top-1: AP ≤ 25 as in Table III). Hence, *camouflaged instance segmentation in-the-wild is still far from being solved, leaving much room for improvement in the future*. These results also indicate the challenges of our CAMO++ dataset.

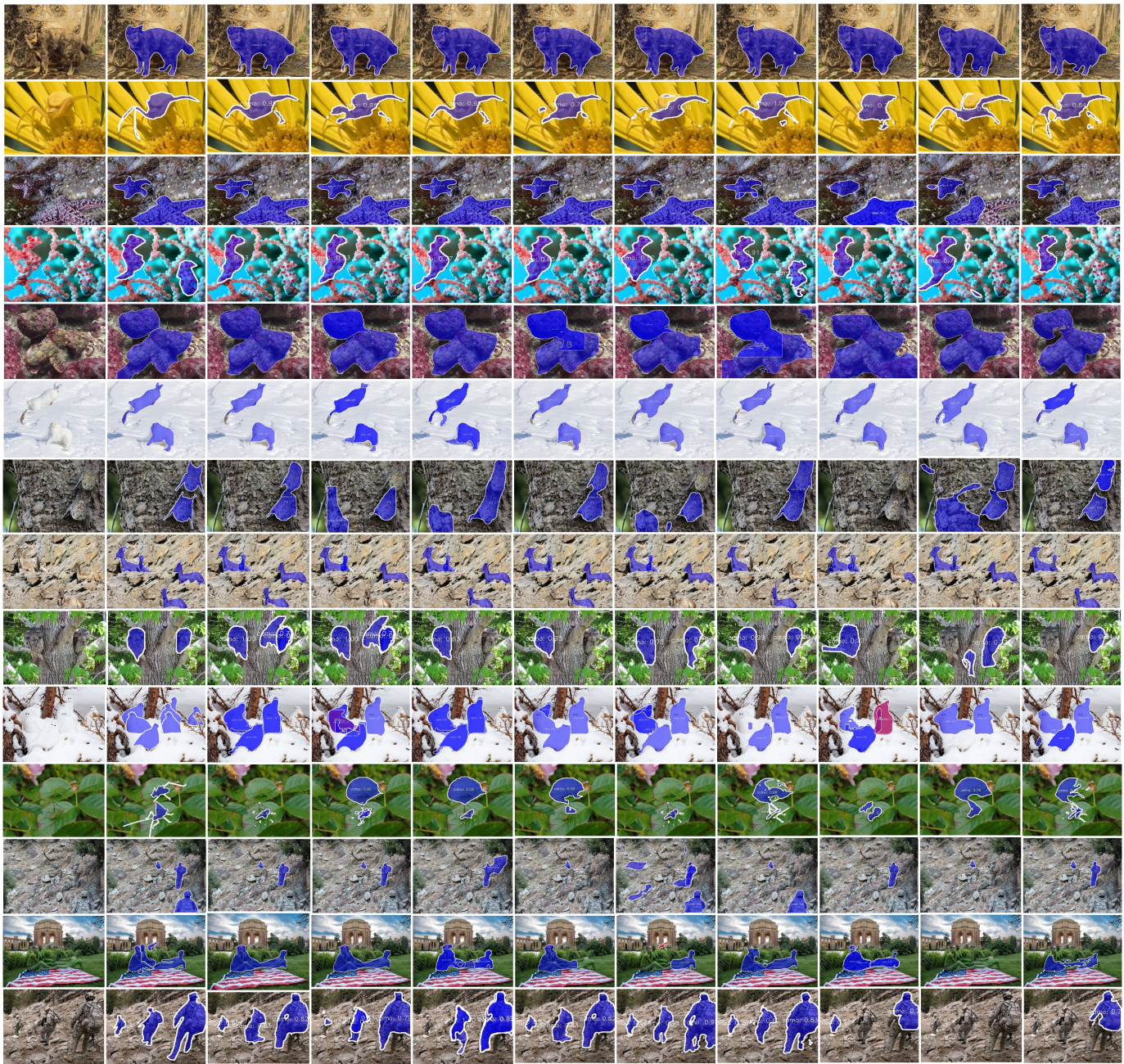


Fig. 14: Comparison of results from different methods. From left to right: the original image is followed by overlaid ground truth and the results of our CFL, Mask RCNN [29], Cascade Mask RCNN [34], MS RCNN [33], RetinaMask [44], YOLACT [38], CenterMask [40], SOLO [47], and BlendMask [39]. Camouflaged instances are shown in blue, and non-camouflaged instances are shown in red. Best viewed in color and with zoom.

VI. DATA ANALYSIS

A. Extra Training Using Non-Camouflage Images

The lack of training data may affect to training camouflage localization and segmentation systems. Existing camouflage works have utilized extra images along with augmented data to improve performance of segmentation. Fan *et al.* [16] combined images from multiple camouflage datasets to train their network. Meanwhile, Li *et al.* [53] recently utilized relation between saliency and camouflage to train a network for joint segmenting salient and camouflaged objects.

In this work, we aim to exploit the ability of utilizing meta knowledge from unseen images (*i.e.*, non-camouflage images with only general objects) to learn camouflaged instances. In particular, we trained instance segmentation methods on a combination of camouflage and non-camouflage images in our CAMO++ dataset.

Table V presents the performance of different methods. We observe that by adding the non-camouflaged instances, the fine-tuned models achieve better performance in segmenting the camouflaged instances. This shows that the training non-

TABLE V: The results of extra training utilizing non-camouflage images. The best results for each type of backbone are shown in **green**, **red**, and **blue**, respectively.

Method	Backbone	Without Extra Training			With Extra Training					
		AP	AP ₅₀	AP ₇₅	AP	AP ₅₀	AP ₇₅	AP	AP ₅₀	AP ₇₅
Mask RCNN [29]	ResNet50-FPN	24.4	52.5	21.1	24.6 (+0.2)	53.3 (+0.8)	20.8 (-0.3)			
Mask RCNN [29]	ResNet101-FPN	23.7	51.5	19.6	26.1 (+2.4)	54.7 (+3.2)	23.4 (+3.8)			
Mask RCNN [29]	ResNeXt101-FPN	31.2	62.7	29.4	31.3 (+0.1)	63.3 (+0.6)	27.7 (-1.7)			
Cascade Mask RCNN [34]	ResNet50-FPN	25.1	51.8	21.9	25.9 (+0.8)	53.4 (+1.6)	22.4 (+0.5)			
Cascade Mask RCNN [34]	ResNet101-FPN	26.7	53.8	23.6	26.9 (+0.2)	54.5 (+0.7)	24.2 (+0.6)			
Cascade Mask RCNN [34]	ResNeXt101-FPN	33.6	66.0	30.7	33.8 (+0.2)	64.8 (-1.2)	33.0 (+2.3)			
MS RCNN [33]	ResNet50-FPN	27.0	54.3	24.5	26.9 (-0.1)	53.2 (-1.1)	25.6 (-1.3)			
MS RCNN [33]	ResNet101-FPN	28.1	55.6	26.2	28.6 (+0.5)	54.6 (-1.0)	27.7 (-0.9)			
MS RCNN [33]	ResNeXt101-FPN	31.0	60.4	29.2	32.9 (+1.9)	62.4 (+2.0)	32.0 (+2.8)			
RetinaMask [44]	ResNet50-FPN	21.5	48.2	17.0	23.5 (+2.0)	50.9 (+2.7)	19.2 (+2.2)			
RetinaMask [44]	ResNet101-FPN	23.5	50.2	19.5	25.4 (+1.9)	54.0 (+3.8)	21.9 (+2.4)			
RetinaMask [44]	ResNeXt101-FPN	25.8	53.1	23.3	28.1 (+2.3)	58.3 (+5.2)	24.4 (+1.1)			
YOLACT [38]	ResNet50-FPN	20.6	41.9	17.5	20.6 (+0)	44.3 (+2.4)	18.2 (+0.7)			
YOLACT [38]	ResNet101-FPN	21.7	42.1	20.0	23.1 (+1.4)	46.9 (+4.8)	20.7 (+0.7)			
CenterMask [40]	ResNet50-FPN	19.7	47.1	13.7	21.3 (+1.6)	50.4 (+3.3)	15.7 (+2.0)			
CenterMask [40]	ResNet101-FPN	23.1	53.3	17.1	24.6 (+1.5)	54.6 (+1.3)	20.2 (+3.1)			
CenterMask [40]	ResNeXt101-FPN	26.6	57.4	23.2	29.9 (+3.3)	62.7 (+5.3)	27.0 (+3.8)			
SOLO [47]	ResNet50-FPN	22.6	46.9	19.3	23.2 (+0.6)	46.9 (+0)	21.1 (+1.8)			
SOLO [47]	ResNet101-FPN	23.8	48.5	21.3	30.5 (+6.7)	60.0 (+11.5)	27.4 (+6.1)			
SOLO [47]	ResNeXt101-FPN	24.3	48.5	22.1	33.3 (+9.0)	62.9 (+14.4)	31.8 (+9.7)			
BlendMask [39]	ResNet50-FPN	21.7	47.4	18.3	25.9 (+4.2)	55.5 (+8.1)	21.6 (-4.3)			
BlendMask [39]	ResNet101-FPN	25.5	53.5	20.6	28.1 (+2.6)	56.5 (+3.0)	25.0 (+4.4)			
Our CFL	ResNet50-FPN	35.2	66.3	32.6	35.7 (+0.5)	65.9 (-0.4)	34.5 (+1.9)			
Our CFL	ResNet101-FPN	36.9	68.2	34.7	37.6 (+0.7)	69.2 (+1.0)	37.8 (+3.1)			
Our CFL	ResNeXt101-FPN	42.8	75.9	44.6	43.7 (+0.9)	74.8 (-1.1)	45.4 (+0.8)			

TABLE VI: Dataset generalization evaluation in camouflaged instance segmentation, using Cascade R-CNN model and AP metric. Columns indicate the generalizability of the training dataset, measured as average value of testing datasets (Higher is better). Rows illustrate the difficulty of the testing dataset, measured as average value of training datasets (Lower is better). The best results are shown in **bold**.

Test Set \ Train Set	Train Set		Mean-Difficulty ↓
	CAMO++	COD [16]	
CAMO++	33.6	23.2	28.4
COD [16]	27.9	31.4	29.7
Mean-Generalizability ↑	30.8	27.3	

camouflaged instances really help boost the performance. Furthermore, once again, our proposed CFL is the top performer. In particular, CFL with ResNeXt101-FPN backbone was boosted thanks to the combined data more significantly than other benchmarked methods. It achieved the best performance (42.8 in AP).

B. Dataset Generalization Evaluation

We investigate generalization of camouflage datasets through cross-dataset evaluation over our CAMO++ and COD [16] datasets. We remark that we used only camouflage images in both these two datasets because the COD dataset does not have ground-truth of non-camouflage images. For fair comparison, we randomly select 1,700 images from training

set and 1,000 images from test set of COD dataset to obtain same number of images in our CAMO++ dataset. We trained Cascade Mask RCNN [34] with backbone ResNeXt101-FPN on each dataset with the same training configuration in Section V-A.

Table VI shows the results of cross-dataset generalization using AP. Each column illustrates results of a model that was trained on one dataset and tested on all datasets, indicating the generalizability of the training dataset. Each row shows the performance of a model that was trained on all datasets and tested on a specific dataset, indicating the difficulty of the testing dataset. As seen in Table VI, our newly constructed CAMO++ dataset is more challenging than COD dataset [16]. In particular, our training images are the most generalized (*e.g.* mean value of 30.8 on the bottom row), which can help to boost the performance on both CAMO++ and COD datasets. Meanwhile, our testing images are also the most difficult (*e.g.* mean value of 28.4 on the right column) due to consists of many challenging cases such as tiny instances, extreme resemblance to the background, distracted instances, occluded and overlapping camouflaged instances (*c.f.* Section V-C4 and Figure 15)

VII. CONCLUSION AND OUTLOOK

In this paper, we study the interesting yet challenging problem, camouflaged instance segmentation. To this end, we collect a large-scale dataset, namely Camouflaged Object Plus Plus (CAMO++). We further provide an in-depth analysis



Fig. 15: Failure cases in camouflaged instance segmentation. From left to right: the original image is followed by overlaid ground truth and the results of our CFL. Camouflaged instances are shown in blue, and non-camouflaged instances are shown in red. From top to bottom are examples of tiny instances, extreme resemblance to the background, occluded and overlapping camouflaged instances, which are immensely challenging even for human. Best viewed in color and with zoom.

on CAMO++ to demonstrate its diversity and complexity. We also proposed a new CFL framework to further improve the performance of camouflaged instance segmentation. We conduct an extensive benchmark for the task of camouflaged instance segmentation. We evaluate state-of-the-art instance segmentation methods in various experimental settings. The results indicate that the existing methods well perform on the problem. In addition, the training non-camouflaged instances really help boost the performance of state-of-the-arts. However, there is still room for the improvement as we discussed in the failure cases. We believe that the CAMO++ dataset can serve as a valuable benchmark for not only the camouflaged instance segmentation task, but also related tasks such as semantic camouflage segmentation, or video camouflaged instance segmentation. We expect that our constructed CAMO++ dataset helps boost the research activities in this field.

In the future, we are exploring the impact of different factors on the given problem. For example, the contextual information may be helpful to detect and segment the camouflaged instance. In addition, we are looking at extending our work into the dynamic scenes such as videos. We would like to investigate the motion information in segmenting the camouflaged instance in the videos.

ACKNOWLEDGMENT

This work was funded by National Science Foundation (NSF) under Grant No. 2025234 and Vingroup Innovation Foundation, Vietnam (VINIF.2019.DA19). We also thank Thanh-An Nguyen, Hoang-Phuc Nguyen-Dinh, and Software Engineering Lab (University of Science, VNU-HCM) for their support in the annotation of the CAMO++ dataset. We gratefully acknowledge NVIDIA for the support of GPU.

REFERENCES

- [1] T.-N. Le, T. V. Nguyen, Z. Nie, M.-T. Tran, and A. Sugimoto, "Anabranh network for camouflaged object segmentation," *Journal of Computer Vision and Image Understanding*, vol. 184, pp. 45–56, 2019.
- [2] S. Singh, C. Dhawale, and S. Misra, "Survey of object detection methods in camouflaged image," *IERI Procedia*, vol. 4, pp. 351 – 357, 2013.
- [3] T.-N. Le, V. Nguyen, C. Le, T.-C. Nguyen, M.-T. Tran, and T. V. Nguyen, "Camouflfinder: Finding camouflaged instances in images," in *AAAI Conference on Artificial Intelligence*, 2021.
- [4] H. A. Qadir, Y. Shin, J. Solhusvik, J. Bergsland, L. Aabakken, and I. Balasingham, "Polyp detection and segmentation using mask r-cnn: Does a deeper feature extractor cnn always perform better?" in *International Symposium on Medical Information and Communication Technology*, 2019.
- [5] F. Ucar and D. Korkmaz, "Covidagnosis-net: Deep bayes-squeezenet based diagnosis of the coronavirus disease 2019 (covid-19) from x-ray images," in *Medical Hypotheses*, 2020.
- [6] H. H. Nguyen, F. Fang, J. Yamagishi, and I. Echizen, "Multi-task learning for detecting and segmenting manipulated facial images and videos," in *International Conference on Biometrics: Theory, Applications and Systems*, 2019.
- [7] H. H. Nguyen, J. Yamagishi, and I. Echizen, "Capsule-forensics: Using capsule networks to detect forged images and videos," in *International Conference on Acoustics, Speech and Signal Processing*, 2019.
- [8] M. Galun, E. Sharon, R. Basri, and A. Brandt, "Texture segmentation by multiscale aggregation of filter responses and shape elements," in *International Conference on Computer Vision*, Oct 2003, pp. 716–723.
- [9] L. Song and W. Geng, "A new camouflage texture evaluation method based on wssim and nature image features," in *International Conference on Multimedia Technology*, Oct 2010, pp. 1–4.
- [10] F. Xue, C. Yong, S. Xu, H. Dong, Y. Luo, and W. Jia, "Camouflage performance analysis and evaluation framework based on features fusion," *Multimedia Tools and Applications*, vol. 75, no. 7, pp. 4065–4082, Apr 2016.
- [11] Y. Pan, Y. Chen, Q. Fu, P. Zhang, and X. Xu, "Study on the camouflaged target detection method based on 3d convexity," *Modern Applied Science*, vol. 5, no. 4, p. 152, 2011.
- [12] Z. Liu, K. Huang, and T. Tan, "Foreground object detection using top-down information based on em framework," *IEEE Transactions on Image Processing*, vol. 21, no. 9, pp. 4204–4217, Sept 2012.
- [13] A. W. P. Sengottuvelan and A. Shanmugam, "Performance of decamouflaging through exploratory image analysis," in *International Conference on Emerging Trends in Engineering and Technology*, July 2008, pp. 6–10.
- [14] J. Yin, Y. Han, W. Hou, and J. Li, "Detection of the mobile object with camouflage color under dynamic background based on optical flow,"

- Procedia Engineering*, vol. 15, no. Supplement C, pp. 2201 – 2205, 2011.
- [15] J. Gallego and P. Bertolino, “Foreground object segmentation for moving camera sequences based on foreground-background probabilistic models and prior probability maps,” in *International Conference on Image Processing*, Oct 2014, pp. 3312–3316.
- [16] D.-P. Fan, G.-P. Ji, G. Sun, M.-M. Cheng, J. Shen, and L. Shao, “Camouflaged object detection,” in *Conference on Computer Vision and Pattern Recognition*, 2020.
- [17] H. Lamdouar, C. Yang, W. Xie, and A. Zisserman, “Betrayed by motion: Camouflaged object discovery via motion segmentation,” in *Asian Conference on Computer Vision*, November 2020.
- [18] J. Zhu, X. Zhang, S. Zhang, and J. Liu, “Inferring camouflage objects by texture-aware interactive guidance network,” in *AAAI*, 2021.
- [19] H. Lamdouar, C. Yang, W. Xie, and A. Zisserman, “Betrayed by motion: Camouflaged object discovery via motion segmentation,” in *Proceedings of the Asian Conference on Computer Vision*, 2020.
- [20] E. L.-M. Pia Bideau, “It’s moving! a probabilistic model for causal motion segmentation in moving camera videos,” in *European Conference on Computer Vision*, 2016.
- [21] P. Skurowski, H. Abdulameer, J. Baszczyk, T. Depta, A. Kornacki, and P. Kozie, “Animal camouflage analysis: Chameleon database,” *Unpublished Manuscript*, 2018.
- [22] J. Yan, T.-N. Le, K.-D. Nguyen, M.-T. Tran, T.-T. Do, and T. V. Nguyen, “Mirronet: Bio-inspired camouflage object segmentation,” *arXiv preprint arXiv:2007.12881*, 2020.
- [23] A. Kirillov, E. Levinkov, B. Andres, B. Savchynskyy, and C. Rother, “Instancecut: from edges to instances with multicut,” in *Conference on Computer Vision and Pattern Recognition*, vol. 3, 2017, p. 9.
- [24] E. Levinkov, J. Uhrig, S. Tang, M. Omran, E. Insafutdinov, A. Kirillov, C. Rother, T. Brox, B. Schiele, and B. Andres, “Joint graph decomposition & node labeling: Problem, algorithms, applications,” in *Conference on Computer Vision and Pattern Recognition*, 2017.
- [25] X. Liang, L. Lin, Y. Wei, X. Shen, J. Yang, and S. Yan, “Proposal-free network for instance-level semantic object segmentation,” *IEEE Transactions on Pattern Analysis and Machine Intelligence*, pp. 1–1, 2017.
- [26] Z. Zhang, S. Fidler, and R. Urtasun, “Instance-level segmentation for autonomous driving with deep densely connected mrfs,” in *Conference on Computer Vision and Pattern Recognition*, 2016, pp. 669–677.
- [27] A. K. Konstantin Sofiiuk, Olga Barinova, “Adaptis: Adaptive instance selection network,” in *International Conference on Computer Vision*, 2019.
- [28] J. Dai, K. He, and J. Sun, “Instance-aware semantic segmentation via multi-task network cascades,” in *Conference on Computer Vision and Pattern Recognition*, 2016.
- [29] K. He, G. Gkioxari, P. Dollár, and R. Girshick, “Mask r-cnn,” in *International Conference on Computer Vision*, 2017, pp. 2980–2988.
- [30] Y. Li, H. Qi, J. Dai, X. Ji, and Y. Wei, “Fully convolutional instance-aware semantic segmentation,” in *Conference on Computer Vision and Pattern Recognition*, 2017.
- [31] S. Ren, K. He, R. Girshick, and J. Sun, “Faster r-cnn: Towards real-time object detection with region proposal networks,” in *Advances in Neural Information Processing Systems*, 2015, pp. 91–99.
- [32] J. Dai, Y. Li, K. He, and J. Sun, “R-fcn: Object detection via region-based fully convolutional networks,” in *Advances in Neural Information Processing Systems*, 2016, pp. 379–387.
- [33] Z. Huang, L. Huang, Y. Gong, C. Huang, and X. Wang, “Mask Scoring R-CNN,” in *Conference on Computer Vision and Pattern Recognition*, 2019.
- [34] Z. Cai and N. Vasconcelos, “Cascade r-cnn: Delving into high quality object detection,” in *Conference on Computer Vision and Pattern Recognition*, 2018.
- [35] S. Liu, L. Qi, H. Qin, J. Shi, and J. Jia, “Path aggregation network for instance segmentation,” in *Conference on Computer Vision and Pattern Recognition*, 2018.
- [36] X. Zhou, D. Wang, and P. Krähenbühl, “Objects as points,” in *arXiv preprint arXiv:1904.07850*, 2019.
- [37] Z. Tian, C. Shen, H. Chen, and T. He, “Fcos: Fully convolutional one-stage object detection,” in *International Conference on Computer Vision*, October 2019.
- [38] D. Bolya, C. Zhou, F. Xiao, and Y. J. Lee, “Yolact: Real-time instance segmentation,” in *International Conference on Computer Vision*, 2019.
- [39] H. Chen, K. Sun, Z. Tian, C. Shen, Y. Huang, and Y. Yan, “Blendmask: Top-down meets bottom-up for instance segmentation,” in *Conference on Computer Vision and Pattern Recognition*, 2020.
- [40] Y. Lee and J. Park, “Centermask: Real-time anchor-free instance segmentation,” in *Conference on Computer Vision and Pattern Recognition*, 2020.
- [41] E. Xie, P. Sun, X. Song, W. Wang, X. Liu, D. Liang, C. Shen, and P. Luo, “Polarmask: Single shot instance segmentation with polar representation,” in *Conference on Computer Vision and Pattern Recognition*, 2020.
- [42] H. Ying, Z. Huang, S. Liu, T. Shao, and K. Zhou, “Embedmask: Embedding coupling for one-stage instance segmentation,” in *Conference on Computer Vision and Pattern Recognition*, 2020.
- [43] X. Chen, R. Girshick, K. He, and P. Dollár, “Tensormask: A foundation for dense object segmentation,” in *International Conference on Computer Vision*, 2019.
- [44] C.-Y. Fu, M. Shvets, and A. C. Berg, “RetinaMask: Learning to predict masks improves state-of-the-art single-shot detection for free,” in *arXiv preprint arXiv:1901.03353*, 2019.
- [45] T.-Y. Lin, P. Goyal, R. Girshick, K. He, and P. Dollár, “Focal loss for dense object detection,” in *International Conference on Computer Vision*, 2017, pp. 2980–2988.
- [46] Z. Tian, C. Shen, and H. Chen, “Conditional convolutions for instance segmentation,” in *European Conference on Computer Vision*, 2020.
- [47] X. Wang, T. Kong, C. Shen, Y. Jiang, and L. Li, “SOLO: Segmenting objects by locations,” in *European Conference on Computer Vision*, 2020.
- [48] A. Gupta, P. Dollar, and R. Girshick, “Lvis: A dataset for large vocabulary instance segmentation,” in *Conference on Computer Vision and Pattern Recognition*, June 2019.
- [49] A. Dosovitskiy, A. Dosovitskiy, L. Beyer, A. Kolesnikov, D. Weissenborn, X. Zhai, T. Unterthiner, M. Dehghani, M. Minderer, G. Heigold, S. Gelly, J. Uszkoreit, and N. Houlsby, “An image is worth 16x16 words: Transformers for image recognition at scale,” in *International Conference on Learning Representations*, 2021.
- [50] K. He, X. Zhang, S. Ren, and J. Sun, “Deep residual learning for image recognition,” in *Conference on Computer Vision and Pattern Recognition*, June 2016, pp. 770–778.
- [51] S. Xie, R. Girshick, P. Dollár, Z. Tu, and K. He, “Aggregated residual transformations for deep neural networks,” in *Conference on Computer Vision and Pattern Recognition*, 2017, pp. 1492–1500.
- [52] T.-Y. Lin, M. Maire, S. Belongie, J. Hays, P. Perona, D. Ramanan, P. Dollár, and C. L. Zitnick, “Microsoft coco: Common objects in context,” in *European Conference on Computer Vision*, 2014, pp. 740–755.
- [53] A. Li, J. Zhang, Y. Lv, B. Liu, T. Zhang, and Y. Dai, “Uncertainty-aware joint salient object and camouflaged object detection,” in *Conference on Computer Vision and Pattern Recognition*, 2021.